# Phase diagram and optical conductivity of $La_{1.8-x}Eu_{0.2}Sr_xCuO_4$

M. Autore,[1] P. Di Pietro,[2] P. Calvani,[2] U. Schade,[3] S. Pyon,[4] T. Takayama,[5] H. Takagi,[4,5] and S. Lupi[6]
[1]*Dipartimento di Fisica and INFN, Università di Roma La Sapienza, Piazzale Aldo Moro 2, I-00185 Roma, Italy*
[2]*CNR-SPIN and Dipartimento di Fisica, Università di Roma La Sapienza, Piazzale Aldo Moro 2, I-00185 Roma, Italy*
[3]*Helmholtz Zentrum für Materialen und Energie, Albert-Einstein-Str. 15, D-12489 Berlin, Germany*
[4]*Department of Physics, University of Tokyo, Tokyo 1130033, Japan*
[5]*Max Planck Institute for Solid State Research, Heisenbergstrasse 1, 70569 Stuttgart, Germany*
[6]*CNR-IOM and Dipartimento di Fisica, Università di Roma La Sapienza, Piazzale Aldo Moro 2, I-00185 Roma, Italy*
(Received 23 October 2013; revised manuscript received 7 June 2014; published 2 July 2014)

$La_{1.8-x}Eu_{0.2}Sr_xCuO_4$ (LESCO) is the member of the 214 family which exhibits the largest intervals among the structural, charge ordering (CO), magnetic, and superconducting transition temperatures. By using new dc transport measurements and data in the literature, we construct the phase diagram of LESCO between $x = 0.8$ and 0.20. This phase diagram has been further probed in ac, by measuring the optical conductivity $\sigma_1(\omega)$ of three single crystals with $x = 0.11$, 0.125, and 0.16 between 10 and 300 K in order to associate the extra-Drude peaks often observed in the 214 family with a given phase. The far-infrared peak we detect in underdoped LESCO is the hardest among them, survives up to room temperature and is associated with charge localization rather than with ordering. At the CO transition for the commensurate doping $x = 0.125$ instead the extra-Drude peak hardens and a pseudogap opens in $\sigma_1(\omega)$, approximately as wide as the maximum superconducting gap of LSCO.

DOI: 10.1103/PhysRevB.90.035102 PACS number(s): 74.25.Gz, 74.72.−h, 74.25.Kc

## I. INTRODUCTION

One of the most interesting issues concerning high-$T_c$ cuprates is the competitive coexistence between superconductivity and charge/magnetic order. This problem dates back to the discovery, in 1988 [1], of a drop in $T_c$ at the commensurate doping $x = 0.125$ in $La_{2-x}Ba_xCuO_4$ (LBCO), and found an explanation with the discovery of commensurate charge and spin order at 1/8 hole doping [2], in form of charge stripes separated by spin walls with no doped holes. It became then clear that static charge and spin ordering competes in cuprates with superconductivity and leads to its partial suppression. Further studies [3–5] on different members of the 214 family, i.e., $A_{2-x}B_xCuO_4$ compounds (where A is a trivalent ion and B a divalent dopant) showed that, upon cooling, such ordering is preceded at a temperature called $T_{d2}$ (see Table I) by a structural transition from the usual low-temperature orthorhombic (LTO) to a low-temperature tetragonal (LTT) phase, through a rotation of the oxygen octahedra surrounding the Cu atoms. The charge ordering process has also important consequences on the infrared response of the 214 compounds. In a recent infrared experiment [6] on $La_{2-x}Ba_xCuO_4$, the existence of localized or gapped excitations was demonstrated at $x = 0.125$ through a transfer of spectral weight from low to higher frequency, which opens a gap in the far infrared below the CO temperature, and builds up a peak at finite frequency (at ∼500 $cm^{-1}$ and ∼300 $cm^{-1}$ broad). Other authors [7–9] had previously reported anomalies in the low-temperature response of different 214 compounds both at commensurate and incommensurate doping, consistently with the results of inelastic neutron scattering [10–12]. The anomalies found in compounds where no static superlattices were observed by conventional diffraction were attributed to fluctuating spin and charge ordering, and are similar to those produced by static ordering. In both cases, for example, an extra-Drude peak appears in the far-infrared (FIR) optical conductivity, which indicates charge localization, and damped spin excitations or "paramagnons" [13] are detected by inelastic x-ray scattering (RIXS). Moreover, in $Bi_2Sr_2CaCu_2O_{8+x}$, scanning tunneling microscopy has revealed both checkerboard charge order in the pseudogap phase [14] and fluctuating charge stripes, which survive in the superconducting dome of the phase diagram. [15]. Fluctuating charge order in cuprates seems then to coexist with, or possibly even to favor, superconductivity. The intriguing implications of this discovery have been widely discussed in the literature (for a review, see, e.g., Ref. [16]).

In an attempt to better understand the interplay between ordering phenomena and superconductivity, another member of the 214 family, $La_{1.8-x}Eu_{0.2}Sr_xCuO_4$ (LESCO) has been investigated in recent years. Therein, below $x = 0.17$, no Meissner effect can be detected [17], while clear indications of antiferromagnetic (AF) order were found for $0 \leqslant x \leqslant 0.014$ by muon spin rotation [18]. Short-range magnetic order was detected in the same experiment for $x > 0.08$. Evidence for stripe formation, with a doping-dependent wave vector, was provided by resonant x-ray diffraction below $T_{\text{CO-diff}} = 80$ K at $x = 1/8$ and below 65 K at $x = 0.15$ [19]. Here also, commensurate order competes with superconductivity, as demonstrated by a recent pump-probe optical experiment. The stripes of LESCO at 1/8 doping were destabilized by a mid-IR pumping of the Cu-O stretching mode. By then probing in the terahertz range both the real and imaginary parts of the optical conductivity, the authors observed that the superconducting state was restored with a strong increase in $T_c$ [20].

The phase diagram of $La_{1.8-x}Eu_{0.2}Sr_xCuO_4$ between $x = 0.08$ and 0.20, is shown in Fig. 1. Here, the structural transition temperature $T_{d2}$ has been estimated from the anomaly in the temperature derivative of the $c$-axis resistivity $d\rho_c/dT$, the magnetic ordering temperature $T_m$ has been taken from Ref. [18], the charge-ordering temperature has been estimated both from diffraction data ($T_{\text{CO-diff}}$), $x = 0.125$ (Ref. [21]) and $x = 0.15$ (Ref. [19]), and for the same samples from a drop in the Hall coefficient versus temperature ($T_{\text{CO-Hall}}$, Ref. [21]).

 

TABLE I. Transition temperatures of three compounds of the 214 family with 0.125 hole doping. $T_{d2}$ refers to the structural LTT-LTO transition, $T_{CO}$ and $T_m$ are the temperatures of charge and spin ordering, respectively, and $T_c$ is the superconducting critical temperature. LESCO exhibits the maximum separation among the above temperatures.

| Compound | $T_{d2}$ (K) | $T_{CO}$ (K) | $T_M$ (K) | $T_c$ (K) |
|---|---|---|---|---|
| $La_{1.48}Nd_{0.4}Sr_{0.12}CuO_4$ [4] | 70 | 60 | 50 | 2 |
| $La_{1.875}Ba_{0.05}Sr_{0.075}CuO_4$ | 55 | 40 [22] | 50 | 10 |
| $La_{1.675}Eu_{0.2}Sr_{0.125}CuO_4$ | 125 [18] | 80 [19] | 45 [23] | 5 |

With respect to the leading member of the family, LSCO, its "superconducting dome" is less pronounced and coexists with an antiferromagnetic phase, which survives at higher temperatures. Optimum doping is achieved for $x = 0.16$, where static charge ordering disappears from the x-ray diffraction spectra. As a result of this phase diagram, in comparison with the other charge-ordered 214 compounds, LESCO exhibits the largest separations among the structural, magnetic, and charge ordering transition temperatures (see Table I). This will make easier, in the present optical study, to separate the effects of long-range charge order from those that can be ascribed to the other transitions, or simply to charge localization effects. Even if LESCO has been studied with different techniques for about fifteen years, to date, it has never been studied by steady-state optical spectroscopy.

## II. EXPERIMENT AND RESULTS

The single crystals of $La_{1.8-x}Eu_{0.2}Sr_xCuO_4$ were all grown at the University of Tokyo using the travelling-solvent floating-zone (TSFZ) technique and were fully characterized as reported in Ref. [21]. The diffraction measurements were performed on the BL19LXU beamline at RIKEN SPring-8, while the resistivity $\rho_c(T)$ and the Hall coefficient $R_H(T)$ of each sample were measured using a standard six-terminal ac technique [21]. Three crystals were selected for the optical measurements: two underdoped samples having $x = 0.11$ ($3.0 \times 3.5 \times 0.3$ mm$^3$ in size) and $x = 0.125$ ($2.0 \times 2.5 \times 0.3$ mm$^3$) and an optimally doped crystal with $x = 0.16$ ($8 \times 4 \times 4$ mm$^3$). Their transition temperatures are reported in Table II.

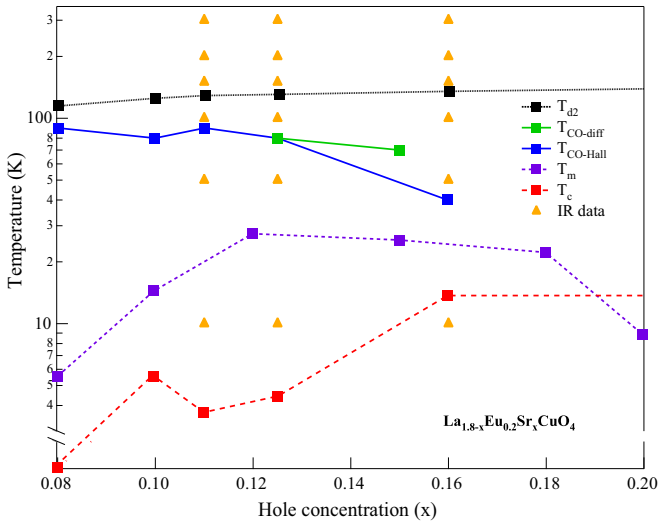


FIG. 1. (Color online) Phase diagram of LESCO. $T_{d2}$ was determined from the anomaly in the temperature derivative of the $c$-axis resistivity $d\rho_c/dT$, the magnetic ordering temperature $T_m$ was taken from Ref. [18], $T_{CO\text{-}diff}$ from Ref. [21] ($x = 0.125$) and Ref. [19] ($x = 0.15$), and $T_{CO\text{-}Hall}$ (determined by the corresponding drop in the Hall coefficient vs temperature) from Ref. [21]. Yellow triangles indicate the low-$T$ optical measurements presented here.

TABLE II. Transition temperatures measured in LESCO single crystals with the same compositions as the three samples considered in the present study. For the employed techniques, refer to the caption of Fig. 1.

| $x$ | $T_{d2}$ (K) | $T_{CO}$ (K) | $T_m$ (K) | $T_c$ (K) |
|---|---|---|---|---|
| 0.11 | 129 | 90 | 20 | 4 |
| 0.125 | 132 | 80 | 30 | 5 |
| 0.16 | 135 | 40 | 25 | 14 |

The reflectivity $R(\omega)$ of the crystals was measured at near-normal incidence, in the $ab$ plane, by a Michelson interferometer from 30 to 20 000 cm$^{-1}$. The $ab$ surface of the crystals was polished with fine powders down to 300 nm, so that the residual roughness was by two orders of magnitude smaller than a typical far-infrared wavelength. In order to avoid that a possible miscut of the $ab$ plane might introduce spurious contributions from the $c$ axis, both in the far and the mid infrared the incident radiation was linearly polarized, using polarizers with 99% rejection rate. The polarizer was rotated while monitoring the sample reflectivity, until any possible trace of the $c$-axis phonons was excluded. This procedure [24] ensures that the $R(\omega)$ is recorded orthogonally to the eventual miscut. The sample was mounted on a cold finger within a helium-flow cryostat. The temperature range was 10–300 K, with an error on temperature of $\pm 2$ K. The reference in the infrared (visible) was a thin gold (silver) layer deposited in situ on the sample. In order to obtain the real part of the optical conductivity $\sigma_1(\omega)$ by standard Kramers-Kronig transformations, $R(\omega)$ was extended to high frequencies using LSCO data from Ref. [25], then extrapolated to $\omega = \infty$ by a $\omega^{-4}$ power law. The extrapolation to zero frequency was instead provided by a Drude-Lorentz fit to the reflectivity, as the standard Hagen-Rubens extrapolation could not be applied in the presence of low-frequency extra-Drude contributions. The $(x,T)$ positions of the spectra are marked by yellow triangles in the phase diagram of Fig. 1.

The reflectivity spectra are shown in Fig. 2 and their temperature variation is concentrated in the far-infrared range. At $\tilde{\omega}_p \simeq 7500$ cm$^{-1}$, they all exhibit a minimum in the near IR at the which is usually indicated as the renormalized, or screened, plasma frequency. However, in metallic cuprates this value cannot be ascribed to the Drude term only, but results from its superposition with a mid-infrared (MIR) band, see below. An interband transition, the Cu-O charge-transfer band, causes the raise in $R(\omega)$ above $\tilde{\omega}_p$.

The real part $\sigma_1(\omega)$ of the optical conductivity, extracted from $R(\omega)$ as reported above, is shown for the three samples

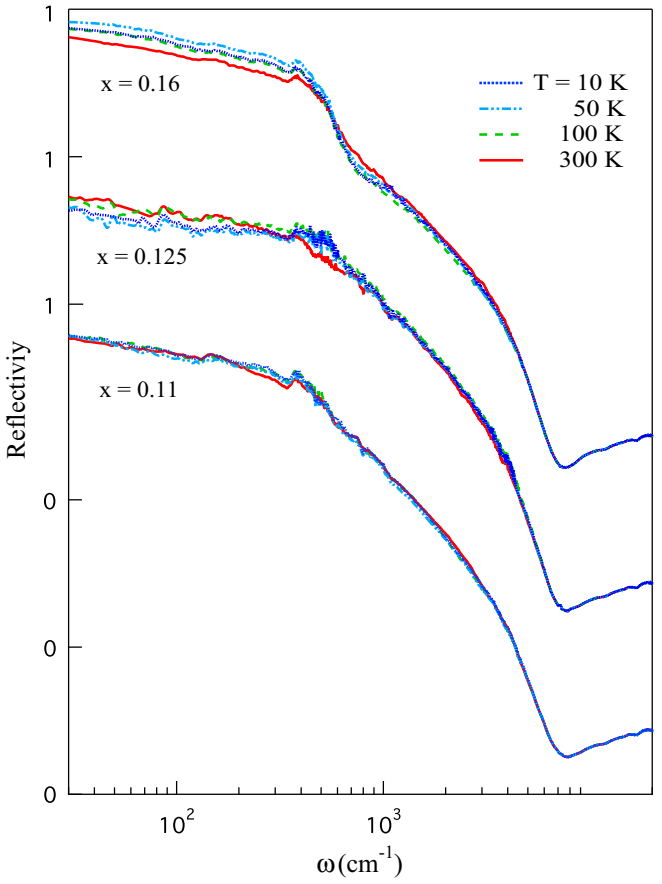


FIG. 2. (Color online) Reflectivity in the *ab* plane for the three $La_{1.8-x}Eu_{0.2}Sr_xCuO_4$ crystals at different temperatures.

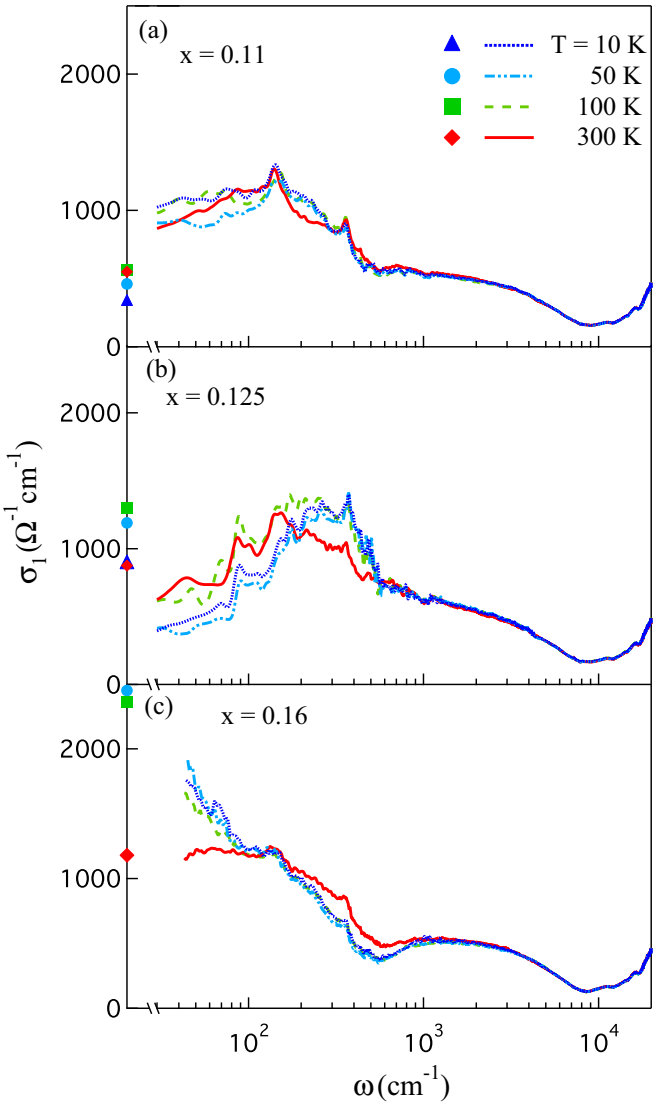


FIG. 3. (Color online) Optical conductivity in the *ab* plane for the $La_{1.8-x}Eu_{0.2}Sr_xCuO_4$ crystals at different temperatures. The dots on the vertical axes correspond to dc resistivity measurements taken along the *a* axis on samples of the same nominal compositions, but not coming from the same batch.

in Fig. 3. DC conductivity data extracted from resistivity measurements along the *a* axis—in an *ac* oriented surface in samples of the same nominal compositions, but not coming from the same batch—are also reported. The agreement is very good for the most metallic sample ($x = 0.16$) and satisfactory for the crystal with $x = 0.11$, given the errors involved both in the both in the absolute resistivity determinations and the far infrared measurements. A larger discrepancy, of about a factor of 2, affects the data for $x = 0.125$. A possible explanation is that further contributions are present in the spectral response of this sample, at frequencies lower than the limit of the present measurements. Those additional absorption lines might be either collective excitations of the charge system [26] or acoustic phonons made active by the Brillouin-zone folding [27] like those observed in the sub-Terahertz spectrum of manganites with commensurate charge ordering. In addition to the charge-transfer band above ~9000 $cm^{-1}$, they all exhibit another feature typical of doped cuprates [28], namely, a broad midinfrared absorption that in LESCO is peaked around 3000 $cm^{-1}$. The origin of this band, which appears in many strongly correlated materials [29–31] upon doping, has been extensively analyzed in the literature. Several explanations for the MIR band have been proposed, which range from electronic states within the charge-transfer gap, to strongly-renormalized scattering rate due to electron-boson coupling [32], to charge-spin polaronic effects [33].

The peculiar features of LESCO appear in the FIR range, where we will focus our discussion. Therein, $\sigma_1(\omega)$ exhibits a conventional Drude-like absorption for the sample at optimum doping ($x = 0.16$) in Fig. 3(c). Its Drude peak gradually narrows upon cooling, with a transfer of spectral weight from high to low frequencies around an isosbestic point situated at $\omega \simeq 150$ $cm^{-1}$ and an appreciable decrease above 150 $cm^{-1}$. A Drude-Lorentz fit (see below) provides a plasma frequency $\omega_p = 4500\,cm^{-1}$, to be compared with $\omega_p = 6100\,cm^{-1}$ in Eu-free LSCO. This helps us to understand another observation, namely that $\sigma_1(\omega)$ for $\omega \to 0$ in Fig. 3(c) is much lower than for LSCO at optimum doping [7]. This may be due to a reduction in the charge density, with respect to the Eu-free compound, despite the fact that Eu was considered for a long time isovalent with La. Finally, despite $T_c$ being 14 K, at $T = 10 \pm 2$ K the opening of a gap is not observed yet. This is probably due to

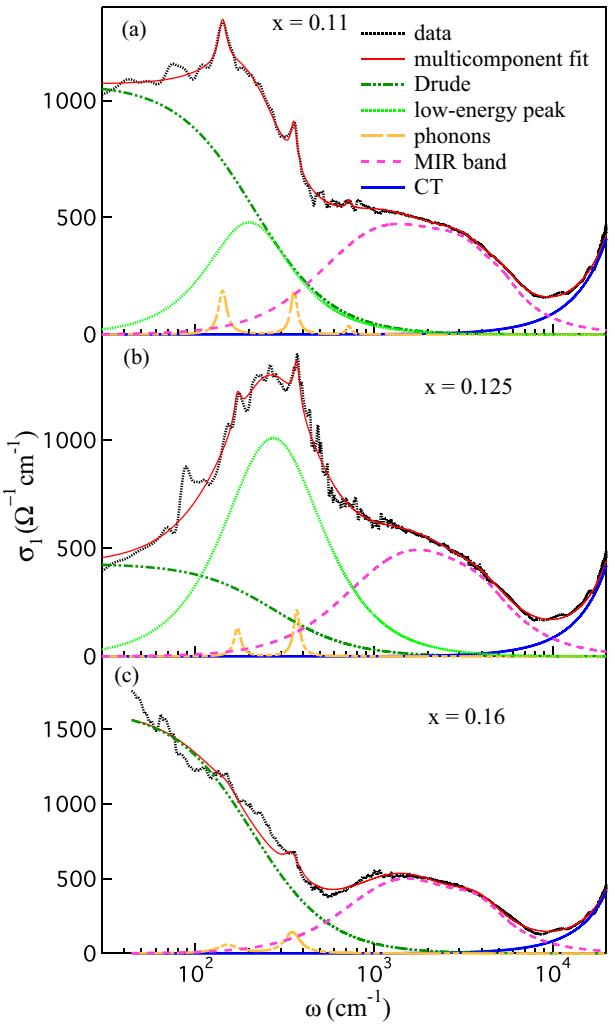


FIG. 4. (Color online) Optical conductivity of the $La_{1.8-x}Eu_{0.2}Sr_xCuO_4$ crystals at 10 K (dotted lines), with the results of Drude-Lorentz fits.

lack of data below 30 $cm^{-1}$, caused by the small size of this crystal.

Both in the $x = 0.11$ and 0.125 samples, at variance with that at optimum doping, $\sigma_1(\omega)$ decreases at any $T$ for $\omega \to 0$. The extra Drude peak responsible for this behavior is clearly shown by the Drude-Lorentz fits reported at 10 K in Figs. 4(a) and 4(b), while it is absent at optimum doping [Fig. 4(c)]. At $x = 0.11$, it is centered around 125 $cm^{-1}$, at $x = 0.125$ around 170 $cm^{-1}$. The fit also distinguishes the $E_u$ phonon peaks of the 214 *ab* plane, increasingly shielded for increasing doping, and the broad MIR band reproduced by the sum of two Lorentzians. Extra Drude peaks at finite frequencies similar to those in Figs. 4(a) and 4(b) were observed in LNSCO [34], underdoped LSCO [7], $La_{1.875}Ba_{0.125-y}Sr_yCuO_4$ (LBSCO) [9], $La_{1.875}Ba_{0.125}CuO_4$ (LBCO) [6] and attributed to charge localization and ordering, either static or dynamic. Figure 5 proposes a comparison among the far-infrared conductivities of LESCO (present experiment), LNSCO [4], and LBSCO [22], at commensurate doping and low temperature. All of them show the extra Drude peak, but the one in LESCO is found at the highest frequency. Consistently with this finding, in

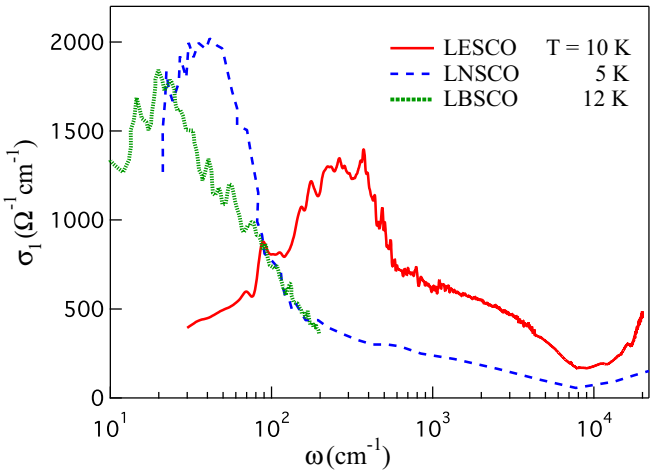


FIG. 5. (Color online) Low-temperature optical conductivity, in the CO phase, of $La_{1.575}Eu_{0.2}Sr_{0.125}CuO_4$, $La_{1.48}Nd_{0.4}Sr_{0.12}CuO_4$ [34], and $La_{1.875}Ba_{0.05}Sr_{0.075}CuO_4$, [22]. $\sigma_1(\omega)$ in $La_{1.48}Nd_{0.4}Sr_{0.12}CuO_4$ and $La_{1.875}Ba_{0.05}Sr_{0.075}CuO_4$ is divided by a factor of 4.

both LESCO samples of Fig. 3 with $x = 0.11$ and 0.125, the peak survives at remarkably high temperatures. They are also higher than all the transition temperatures reported in Table I for $x = 0.125$ and in the phase diagram of Fig. 1. Therefore the charge carriers associated with the extra-Drude peak in these compounds are localized even in the absence of long-range order. For $x = 0.11$, the peak is approximately independent of temperature. For $x = 0.125$ instead, it hardens considerably below the CO transition at 80 K, indicating that it is such shift, not the appearance of the peak itself, which is related to long-range ordering.

To better follow the process induced by CO in LESCO, we have plotted in Fig. 6 the variation of the optical conductivity between different temperatures and room temperature for both underdoped crystals in the far infrared. While at $x = 0.11$, as anticipated previously, there is no appreciable change in the whole temperature range, the sample with commensurate doping $x = 0.125$ exhibits a depletion in $\sigma(\omega)$ below 200 $cm^{-1}$ which indicates the opening of a pseudogap. This effect starts at 100 K, below $T_{d2} = 132$ K, as indicated by a clear change of slope in $\sigma_1(\omega)$, between 200 and 100 K, for $\omega \to 0$. The opening continues below $T_{CO} = 80$ K, through a transfer of spectral weight towards higher frequencies. One should remark that the direct observation of a pseudogap in $\sigma_1(\omega)$ is possible along the $c$ axis [35] but rather unusual for the *ab* plane of cuprates, where such phenomena are typically detected in the carrier relaxation rate $\Gamma(\omega)$, after the application of an extended Drude model [32]. Here, the latter analysis provides meaningful results neither in the optimally doped sample [Fig. 3(b)] due to the sharp separation between the Drude term and the $T$-independent MIR band, nor in the other samples by the peaks at finite frequencies [see Figs. 3(a) and 3(c)]. In the latter two cases, they make $\tau^{-1}(\omega)$ comparable with $\omega$, in contrast with basic assumptions of the Fermi liquid model. One may finally remark that the width of the present CO gap (200 $cm^{-1}$) is comparable with that of the optical gap in superconducting LSCO. This similarity in the energy scale between commensurate charge/spin ordering

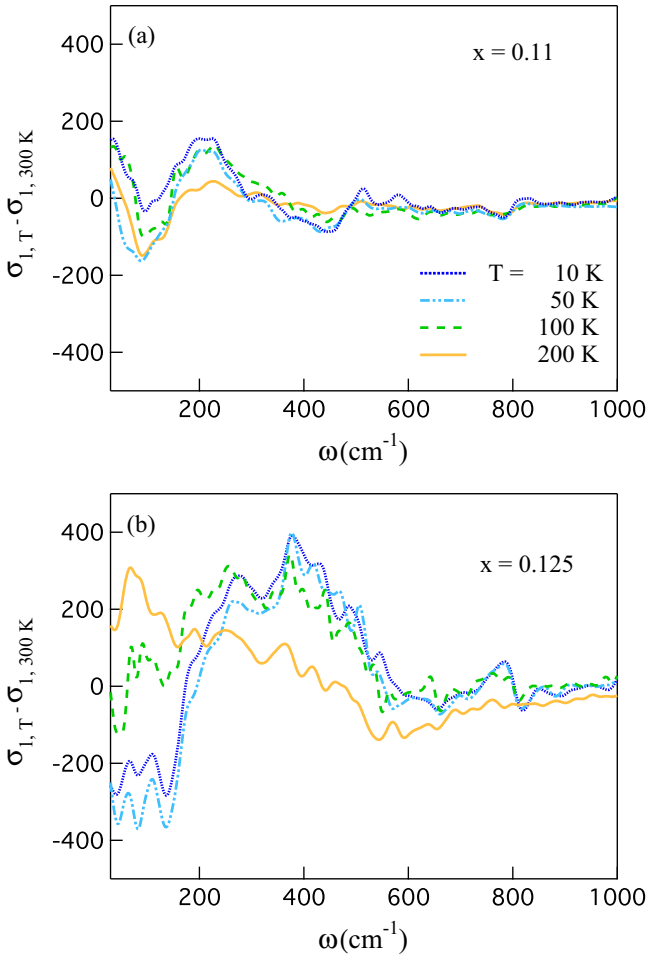


FIG. 6. (Color online) Variation of the optical conductivity between different temperatures $T$ and 300 K, for the underdoped $La_{1.8-x}Eu_{0.2}Sr_xCuO_4$ crystals.

and superconductivity substantiates the observation that the former effect can compete with the Cooper pair formation energy and therefore dramatically reduce $T_c$ in the cuprates of the 214 family.

## III. CONCLUSION

This work reports an optical investigation of Eu-doped LSCO around the 1/8 commensurate doping. This member of the 214 family has been selected for its peculiar phase diagram, where the transitions between different structural, electronic, and magnetic phases are well separated in temperature. Eu doping produces in LSCO a pronounced reduction of low-energy conductivity, which basing on the present infrared measurements can be ascribed mainly to a reduction in the plasma frequency and then in the concentration of the free carriers, despite Eu being considered isovalent with La. In the underdoped samples with $x = 0.11$ and 0.125, a FIR peak is observed at $\omega \sim 200$ cm$^{-1}$, which is similar to those detected in the other 214 compounds which exhibit charge and spin ordering. Nevertheless, here the peak survives at temperatures much higher than both $T_{CO} = 80$ K and $T_{d2} = 132$ K, indicating that it is related to charge localization rather then to long-range ordering. Only in the commensurate $x = 0.125$ sample we find evidence for a strong effect below $T_{CO}$. This is the opening of a pseudogap about 200 cm$^{-1}$ wide, caused by a pronounced hardening of the above peak, with a recovery of the sum rule around 600 cm$^{-1}$. The observation is very similar to that reported in Fig. 15 of Ref. [6] for $La_{2-x}Ba_xCuO_4$. Finally, we have found that, in LESCO, the pseudogap which opens at $x = 0.125$ and the superconducting gap observed at optimum doping are on the same energy scale. This provides further evidence that a strong competition can arise at low temperature between charge ordering and Cooper pair formation in the cuprates of the 214 family.

[1] A. R. Moodenbaugh, Y. Xu, M. Suenaga, T. J. Folkerts, and R. N. Shelton, Phys. Rev. B **38**, 4596 (1988).
[2] J. M. Tranquada, B. J. Sternlieb, J. D. Axe, Y. Nakamura, and S. Uchida, Nature (London) **375**, 561 (1995).
[3] M. Fujita, H. Goka, K. Yamada, J. M. Tranquada, and L. P. Regnault, Phys. Rev. B **70**, 104517 (2004).
[4] J. M. Tranquada, J. D. Axe, N. Ichikawa, A. R. Moodenbaugh, Y. Nakamura, and S. Uchida, Phys. Rev. Lett. **78**, 338 (1997).
[5] N. Ichikawa, S. Uchida, J. M. Tranquada, T. Niemöller, P. M. Gehring, S.-H. Lee, and J. R. Schneider, Phys. Rev. Lett. **85**, 1738 (2000).
[6] C. C. Homes, M. Hucker, Q. Li, Z. J. Xu, J. S. Wen, G. D. Gu, and J. M. Tranquada, Phys. Rev. B **85**, 134510 (2012).
[7] A. Lucarelli, S. Lupi, M. Ortolani, P. Calvani, P. Maselli, M. Capizzi, P. Giura, H. Eisaki, N. Kikugawa, T. Fujita, M. Fujita, and K. Yamada, Phys. Rev. Lett. **90**, 037002 (2003).
[8] W. J. Padilla, M. Dumm, Seiki Komiya, Yoichi Ando, and D. N. Basov, Phys. Rev. B **72**, 205101 (2005).
[9] M. Ortolani, P. Calvani, S. Lupi, U. Schade, A. Perla, M. Fujita, and K. Yamada, Phys. Rev. B **73**, 184508 (2006).
[10] R. J. Birgeneau, Y. Endoh, K. Kakurai, Y. Hidaka, T. Murakami, M. A. Kastner, T. R. Thurston, G. Shirane, and K. Yamada, Phys. Rev. B **39**, 2868 (1989).
[11] S-W. Cheong, G. Aeppli, T. E. Mason, H. Mook, S. M. Hayden, P. C. Canfield, Z. Fisk, K. N. Clausen, and J. L. Martinez, Phys. Rev. Lett. **67**, 1791 (1991).
[12] K. Yamada, C. H. Lee, K. Kurahashi, J. Wada, S. Wakimoto, S. Ueki, H. Kimura, Y. Endoh, S. Hosoya, G. Shirane, R. J. Birgeneau, M. Greven, M. A. Kastner, and Y. J. Kim, Phys. Rev. B **57**, 6165 (1998).
[13] M. P. M. Dean, G. Dellea, M. Minola, S. B. Wilkins, R. M. Konik, G. D. Gu, M. Le Tacon, N. B. Brookes, F. Yakhou-Harris, K. Kummer, J. P. Hill, L. Braicovich, and G. Ghiringhelli, Phys. Rev. B **88**, 020403 (2013).
[14] W. D. Wise, M. C. Boyer, K. Chatterjee, T. Kondo, T. Takeuchi, H. Ikuta, Y. Wang, and E. W. Hudson, Nat. Phys. **4**, 696 (2008).

[15] C. V. Parker, P. Aynajian, E. H. da Silva Neto, A. Pushp, S. Ono, J. Wen, Z. Xu, G. Gu, and A. Yazdani, Nature (London) **468**, 677 (2010).
[16] S. A. Kivelson, I. P. Bindloss, E. Fradkin, V. Oganesyan, J. M. Tranquada, A. Kapitulnik, and C. Howald, Rev. Mod. Phys. **75**, 1201 (2003), and references therein.
[17] V. Kataev, B. Rameev, A. Validov, B. Büchner, M. Hücker, and R. Borowski, Phys. Rev. B **58**, R11876 (1998).
[18] H.-H. Klauss, W. Wagener, M. Hillberg, W. Kopmann, H. Walf, F. J. Litterst, M. Hücker, and B. Büchner, Phys. Rev. Lett. **85**, 4590 (2000).
[19] Jörg Fink, Enrico Schierle, Eugen Weschke, Jochen Geck, David Hawthorn, Viktor Soltwisch, Hiroki Wadati, Hsueh-Hung Wu, Hermann A. Dürr, Nadja Wizent, Bernd Büchner, and George A. Sawatzky, Phys. Rev. B **79**, 100502 (2009).
[20] D. Fausti, R. I. Tobey, N. Dean, S. Kaiser, A. Dienst, M. C. Hoffmann, S. Pyon, T. Takayama, H. Takagi, and A. Cavalleri, Science **331**, 189 (2011).
[21] O. Cyr-Choiniefe, R. Daou, F. Laliberte, D. LeBoeuf, N. Doiron-Leyraud, J. Chang, J.-Q. Yan, J.-G. Cheng, J.-S. Zhou, J. B. Goodenough, S. Pyon, T. Takayama, H. Takagi, Y. Tanaka, and L. Taillefer, Nature (London) **458**, 743 (2009).
[22] Y.-J. Kim, G. D. Gu, T. Gog, and D. Casa, Phys. Rev. B **77**, 064520 (2008).
[23] M. Hücker *et al.*, Physica C **460–462**, 170 (2007).
[24] M. Ortolani, S. Lupi, P. Calvani, and P. Maselli, J. Opt. Soc. Am. B **22**, 1994 (2005).
[25] S. Uchida, T. Ido, H. Takagi, T. Arima, Y. Tokura, and S. Tajima, Phys. Rev. B **43**, 7942 (1991).
[26] A. Nucara, P. Maselli, P. Calvani, R. Sopracase, M. Ortolani, G. Gruener, M. Cestelli Guidi, U. Schade, and J. García, Phys. Rev. Lett. **101**, 066407 (2008).
[27] E. Zhukova, B. Gorshunov, T. Zhang, Dan Wu, A. S. Prokhorov, V. I. Torgashev, E. G. Maksimov, and M. Dressel, Europhys. Lett. **90**, 17005 (2010).
[28] S. Lupi, P. Maselli, M. Capizzi, P. Calvani, P. Giura, and P. Roy, Phys. Rev. Lett. **83**, 4852 (1999).
[29] L. Baldassarre, A. Perucchi, D. Nicoletti, A. Toschi, G. Sangiovanni, K. Held, M. Capone, M. Ortolani, L. Malavasi, M. Marsi, P. Metcalf, P. Postorino, and S. Lupi, Phys. Rev. B **77**, 113107 (2008).
[30] S. Lupi, L. Baldassarre, B. Mansart, A. Perucchi, A. Barinov, P. Dudin, E. Papalazarou, F. Rodolakis, J.-P. Rueff, J.-P. Itie, S. Ravy, D. Nicoletti, P. Postorino, P. Hansmann, N. Parragh, A. Toschi, T. Saha-Dasgupta, O. K. Andersen, G. Sangiovanni, K. Held, and M. Marsi, Nat. Commun. **1**, 105 (2010).
[31] A. Perucchi, C. Marini, M. Valentini, P. Postorino, R. Sopracase, P. Dore, P. Hansmann, O. Jepsen, G. Sangiovanni, A. Toschi, K. Held, D. Topwal, D. D. Sarma, and S. Lupi, Phys. Rev. B **80**, 073101 (2009).
[32] For extensive reviews, see T. Timusk and B. Statt, Rep. Prog. Phys. **62**, 61 (1999); D. N. Basov and T. Timusk, Rev. Mod. Phys. **77**, 721 (2005).
[33] G. De Filippis, V. Cataudella, V. Marigliano Ramaglia, and C. A. Perroni, Phys. Rev. B **72**, 014307 (2005).
[34] M. Dumm, D. N. Basov, Seiki Komiya, Yasushi Abe, and Yoichi Ando, Phys. Rev. Lett. **88**, 147003 (2002).
[35] M. Reedyk, T. Timusk, Y.-W. Hsueh, B. W. Statt, J. S. Xue, and J. E. Greedan, Phys. Rev. B **56**, 9129 (1997).